

Amplification of Ultrashort Laser Pulses by Brillouin Backscattering in Plasmas

S. Weber,^{1,2} C. Riconda,³ L. Lancia,^{4,5} J.-R. Marquès,⁶ G. A. Mourou,¹ and J. Fuchs⁶

¹*IZEST, Ecole Polytechnique–CEA, 91128 Palaiseau, France*

²*Institute of Physics of the ASCR, ELI-Beamlines, 18221 Prague, Czech Republic*

³*LULI, Université Pierre et Marie Curie-Ecole Polytechnique-CNRS-CEA, 75252 Paris, France*

⁴*SAPIENZA, University of Rome, Dipartimento SBAI, 00161 Rome, Italy*

⁵*INFN-Sezione Roma-SAPIENZA, University of Rome, 00185 Rome, Italy*

⁶*LULI, CNRS-Ecole Polytechnique-Université Pierre et Marie Curie-CEA, 91128 Palaiseau, France*

(Received 9 December 2012; published 31 July 2013)

Plasma media, by exciting Raman (electron) or Brillouin (ion) waves, have been used to transfer energy from moderately long, high-energy light pulses to short ones. Using multidimensional kinetic simulations, we define here the optimum window in which a Brillouin scheme can be exploited for amplification and compression of short laser pulses over short distances to very high power. We also show that shaping the plasma allows for increasing the efficiency of the process while minimizing other unwanted plasma processes. Moreover, we show that, contrary to what was traditionally thought (i.e., using Brillouin in gases for nanosecond pulse compression), this scheme is able to amplify pulses of extremely short duration.

DOI: [10.1103/PhysRevLett.111.055004](https://doi.org/10.1103/PhysRevLett.111.055004)

PACS numbers: 52.38.Dx, 52.35.Fp, 52.38.Bv, 52.65.Rr

Since the conception of the laser, there has been a constant push towards increasing the power and focused intensity of the produced light pulses. Doing so has indeed proven to open many new possibilities for fundamental science (e.g., nonlinear optics, compact particle acceleration) and applications (e.g., nonthermal precision machining, medicine). Moreover, with higher intensity lasers, one can produce even shorter pulses through nonlinear effects [1], giving access to faster processes [2].

Fast progress on the increase of laser power has relied on solid state optics using techniques such as CPA (chirped pulse amplification) [3] or OPCPA (optical parametric chirped pulse amplification) [4]. These optics are, however, limited by a very low damage threshold [5] of the order of a few 100 mJ per cm². Further progress relies on increasing the beam diameter, which increases the costs for the optics. By contrast, amplifiers based on plasma gratings resulting from laser-matter interaction, a medium unaffected by damage and extremely compact, present many advantageous properties that allow us to directly amplify extremely short laser pulses. The scheme, which is limited by strong nonlinear effects as will be discussed below, exploits energy transfer, mediated by the plasma, between a long, high energy, pump pulse and a short, low-intensity seed pulse. It can also be thought of as the scattering of one electromagnetic wave onto the plasma wave in order to reinforce or amplify the other electromagnetic wave. The plasma wave can be either an electronic (Raman) or an ionic wave (Brillouin). The coupling requires precise momentum ($k_{\text{pump}} = k_{\text{seed}} + k_{\text{plasma}}$) and energy ($\omega_{\text{pump}} = \omega_{\text{seed}} + \omega_{\text{plasma}}$) conservation conditions. Both processes can be described by similar coupled equations [6,7], although they require quite different plasma and laser conditions.

Much effort has been put in the Raman amplification of short pulses [7–10], producing up to 3 mJ, 50 fs, 10¹⁶ W/cm² in a plasma channel [11]. Extrapolating these results, amplification of centimeter wide laser beams to 10¹⁸ W/cm² was studied [12]. However, (1) this requires wide and long (> 10 mm) quasihomogeneous plasmas [8,12,13], (2) since ω_{plasma} depends on the plasma density, any change in the latter strongly affects the process efficiency, and finally (3) the large frequency difference between ω_{pump} and ω_{seed} implies that one or the other has to be at a precise frequency that does not correspond to standard laser technologies. In general stimulated Raman backscattering (SRS) is favored by low temperatures in conjunction with very low plasma densities.

Brillouin amplification has been considered in the past for fluids and gases. However, due to the characteristic phonon period of the order of 100 ps and the ionization breakdown of the material its use is very limited (see [6] and references therein). Using stimulated Brillouin backscattering (SBS) in plasmas avoids the breakdown and reduces the characteristic time scale to the ion-acoustic wave period of the order of a few picoseconds. Further improvement is obtained by SBS amplification in the only recently studied strong-coupling (sc) regime [6,14]. It is suited for very short pulses and eases considerably some of the following technical difficulties: (1) pump and seed can be at the same frequency, in fact the amplification process is self-organizing by selecting the good frequencies, (2) the coupling is set not by a natural resonant mode but by a forced nonlinear oscillation, and since the energy transfer is fast, the interaction length is short (sub-mm), (3) the process is stable with respect to frequency mismatches associated to density inhomogeneities and it is also not

very sensitive to the electron temperature, (4) full pump depletion is easily obtained. However, when the seed pulse duration gets very short, i.e., its spectrum very wide, and high seed intensities are used, a mixing between SBS and SRS mechanisms can take place and the two can contribute simultaneously to the amplification process (see below). Concentrating on this scheme, and using multidimensional simulations, we study in this Letter the range of laser and plasma parameters to be used in order to amplify light pulses over short distances to very high power. In particular, we establish that shaping the plasma allows for increasing the efficiency of the process while minimizing other unwanted plasma processes. We also show that, contrary to what was traditionally thought, this scheme is able to amplify pulses of extremely short duration. This allows us to foresee, beyond the conditions of present-day experiment, the way to produce extremely high power light pulses generation in mm-scale plasma amplifiers, in line with the goals of the IZEST initiative [15,16]. Let us first evaluate the most appropriate set of laser and plasma parameters for optimal Brillouin amplification and beat competing processes. In order to (1) avoid filamentation of pump or seed of duration $\tau_{p,s}$ we need $\tau_{p,s}/\tau_{\text{fil}} < 1$, where $1/(\tau_{\text{fil}}\omega_0) = \gamma_{\text{fil}}/\omega_0 \approx 10^{-5} I_{14} \lambda_0^2 [\mu\text{m}] (n_e/n_c)$ is the filamentation growth rate [17]. Here I_{14} is the intensity in units of 10^{14} W/cm² and $n_c = 10^{21}/\lambda_0^2 [\mu\text{m}]$ is the critical density. This puts an upper limit to the pump pulse duration and, hence, to the amplifier length. For typical parameters that will be justified below, i.e., 10^{16} W/cm² laser beams and $0.05 n_c$ plasma, the maximum τ_p is then of the order of 10 ps, and the plasma amplifier is up to 3 mm long. These numbers are both technologically well suited, and allow, as will be shown, high amplification. We also want (2) the amplification to be efficient, which means $\tau_s/\tau_{\text{sc}} \geq 1$, where $1/(\tau_{\text{sc}}\omega_0) = \gamma_{\text{sc}}/\omega_0 = 3.6 \times 10^{-2} (I_{14} \lambda_0^2 [\mu\text{m}])^{1/3} (Zm_e/m_i)^{1/3} (n_e/n_c)^{1/3}$ is the growth rate for the strong-coupling SBS instability [18]. Furthermore, we want to (3) avoid wave breaking, which can induce fracturing of the seed (as observed in the simulations), which means $\tau_s/\tau_{\text{wb}} < 1$ where $\tau_{\text{wb}}\omega_0 \approx 1.2 \times 10^2 \sqrt{m_i/2m_e} / \sqrt{I_{14} \lambda_0^2 [\mu\text{m}]} [18]$. From these two last conditions, a limiting intensity can be derived by setting $\tau_{\text{sc}} \sim \tau_{\text{wb}}$, which gives $a_{\text{max}} = v_{\text{osc}}/c \approx (m_i/Zm_e)^{1/2} n_e/n_c$ with $v_{\text{osc}} = eE_0/m_e\omega_0$ the quiver velocity of the electron in the laser electric field E_0 . For a $0.05 n_c$ plasma, this corresponds to a highest obtainable intensity $\sim 0.7 \times 10^{18}$ W/cm². For the SRS-amplification scheme, using densities of the same order of magnitude, the breaking of the electron plasma waves takes place at much lower intensities [19]. The characteristic times derived above are plotted as a function of plasma density in Fig. 1. Since we aim at reaching relativistic intensities for the amplified seed, condition (1) is quite stringent as it implies $\tau_s < \tau_{\text{fil}}$ at 10^{18} W/cm². One observes that τ_{fil}

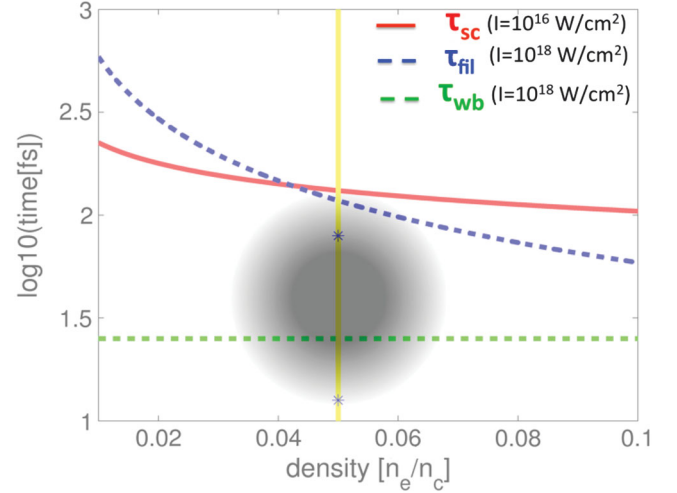


FIG. 1 (color). Characteristic time scales of the various processes at play within the plasma amplifier, as a function of the operating plasma density. The curves were calculated using ion mass $m_i = 3600 m_e$, charge $Z = 1$, and wavelength $\lambda_0 = 1 \mu\text{m}$.

(at 10^{18} W/cm²) is smaller than τ_{sc} (at 10^{16} W/cm², as dictated by the pump), except in the very low density region where coupling is very inefficient. By operating at $\tau_s < \tau_{\text{sc}}$, we nevertheless find, even if condition (2) is not fulfilled, that amplification is successful. The closer τ_s is to τ_{sc} , the more efficient energy transfer is. Reducing τ_s in order to satisfy condition (3) allows us to reach the highest intensity. These two optimal cases will be illustrated in the following by considering two seed durations (80 fs and 13 fs), and are represented in Fig. 1 by star markers. The overall optimum operating window is illustrated in Fig. 1 by a shaded circle (the darker the circle, the better the amplification): high density implies filamentation, very low density gives weak coupling, very short pulses suffer from low-energy transfer efficiency, and too long pulses are submitted to wave breaking. The Raman backscattering instability has a growth rate [18] given as $\gamma_{\text{SRS}}/\omega_0 \approx 4.3 \times 10^{-3} (I_{14} \lambda_0^2)^{1/2} (n_e/n_c)^{1/4}$. For the above parameters this results in $1/\gamma_{\text{SRS}} \approx 25$ fs and SRS can definitely be excited during the amplification process. However, electron plasma waves are strongly Landau damped at high temperatures and the losses are small. In addition SRS is affected by nonhomogeneous plasma profiles whereas SBS is robust (see below). Now that the parameters for optimal SBS amplification have been identified, we need to further evaluate its quality with respect to the following issues: (1) how short the seed pulse can be, (2) the maximum energy transfer, and (3) the role of the plasma profile. For this, two-dimensional first-principle kinetic simulations were performed using the particle-in-cell (PIC) approach [20]. The noise in a PIC code is several orders of magnitude larger than the thermal noise in a plasma. Parametric instabilities grow on the noise and their initial exponential growth is therefore exaggerated. However, in

the amplification simulations presented here the sc-SBS instability responsible for the energy transfer is controlled by the seed pulse and not by the noise and is represented realistically. By contrast, spurious SRS backscattering and filamentation of the pump are most likely overestimated which plays in favor of the amplification process in reality. Therefore the PIC approach represents a worst case scenario. In the standard experimental configuration used up to now for plasma amplifiers [14] the plasma has a trapezoidal form motivated by gas-jet profiles, composed of a $240\ \mu\text{m}$ plateau at density $0.05\ n_c$ and a $240\ \mu\text{m}$ ramp on each side. The total length of the plasma amplifier is therefore $720\ \mu\text{m}$. The plasma is composed of electrons and ions with charge $Z = 1$, mass $m_i = 3600m_e$ and an electron and ion temperature of $T_e = 500\ \text{eV}$ and $T_i = 50\ \text{eV}$, respectively. The wavelength is $\lambda_0 = 1\ \mu\text{m}$. The pump has a fixed spatial FWHM of $\sim 32\ \mu\text{m}$, a duration of $3.5\ \text{ps}$, and an intensity of $10^{16}\ \text{W}/\text{cm}^2$. The seed-pulse spatial size is a bit smaller than the pump (FWHM of $\sim 22\ \mu\text{m}$) in order to be fully contained by the pump volume. Taking into account the overlap volume between pump and seed, the pump can provide at most $\sim 100\ \text{mJ}$ of energy. Once the seed intensity supercedes the pump intensity, $I_s(t > I_p)$, the crucial part of the amplification process sets in. Simulations show that the initial part of the amplification process from $10^{14} \dots 10^{15}\ \text{W}/\text{cm}^2$ up to $10^{17}\ \text{W}/\text{cm}^2$ poses no problem and can be performed with an efficiency of 20%–30%. For this reason we consider here simulations with an initial seed pulse intensity of $10^{17}\ \text{W}/\text{cm}^2$. For this intensity the initial energy content of the seed is ~ 7.5 and $\sim 46\ \text{mJ}$ for seed pulse durations of 13 and 80 fs, respectively. The simulations were performed with the two-dimensional relativistic code EMI2D using open boundary conditions for the lasers and recycling for the particles.

We performed a large number of simulations, out of which we will discuss here two cases which exemplify two strategies: amplifying the shortest pulses, or

maximizing the energy extraction by the seed pulse (illustrated in Fig. 2). Figures 2(a) and 2(b) show that SBS amplification of an extremely short pulse (13 fs) behaves well, the seed pulse increasing its intensity from $10^{17}\ \text{W}/\text{cm}^2$ to $1.5 \times 10^{18}\ \text{W}/\text{cm}^2$ over $0.7\ \text{mm}$. At the same time the temporal FWHM of the seed is compressed down to 8 fs. In the low-density part, $x < 1000\ k_0^{-1}$, the coupling becomes inefficient. The energy in the seed pulse is conserved and the drop in intensity is due to diffraction [Fig. 2(b)]. However, since $\tau_s < \tau_{sc}$ the efficiency of energy transfer remains low (6%, i.e., $\sim 6\ \text{mJ}$), and most of the pump energy is wasted. Also, since a sufficiently high intensity is needed to excite the plasma grating, only the centre of the transverse seed profile gets amplified at the expense of the wings: the transverse FWHM gets reduced from the initial value of $22\ \mu\text{m}$ to $\sim 5\ \mu\text{m}$. Thus the seed pulse would be better transversally profiled as strongly super-Gaussian in order to improve its energy extraction. Nevertheless, as τ_s is smaller even than τ_{wb} at $10^{18}\ \text{W}/\text{cm}^2$, the order of the limiting value a_{max} has been reached. Keeping the natural constraint of a Gaussian profile, we need to increase the pulse duration to increase the energy transfer. By using 80 fs for the seed, the energy efficiency goes up to 31% (i.e., $\sim 31\ \text{mJ}$), although the final intensity reached is only $\sim 4 \times 10^{17}\ \text{W}/\text{cm}^2$. Again a pulse compression, from 80 fs down to 53 fs, is taking place. As the final intensity value is below a_{max} , amplification is not affected by wave breaking.

Figure 3 displays the temporal structure and the spectra of the amplified seed pulses from Fig. 2 once they have left the plasma amplifier. For the shortest pulse of 13 fs the spectra is very broad and the centre is downshifted far beyond what would be expected due to the strong coupling coefficient γ_{sc} [21]. While amplification starts out as a pure sc-SBS process, towards the end of amplification when approaching relativistic intensities the Brillouin and Raman mode start to mix which contributes to the broadening of the frequency structure while at the same time downshifting the spectrum [Fig. 3(a)] [21,22]. For this very

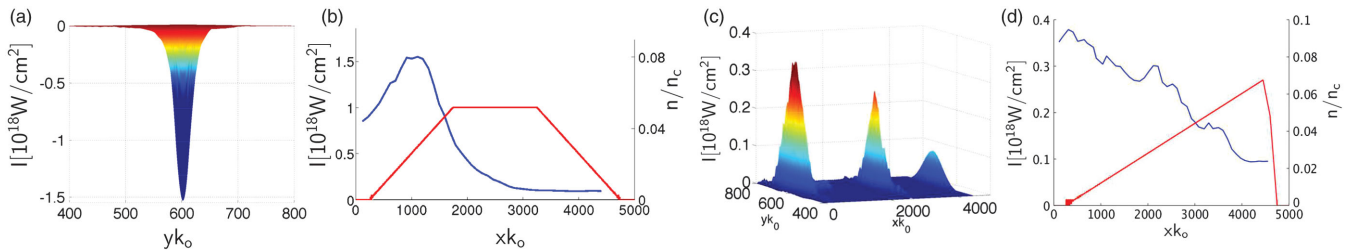


FIG. 2 (color). Amplification of a seed pulse of initial intensity $10^{17}\ \text{W}/\text{cm}^2$ by a pump pulse of intensity $10^{16}\ \text{W}/\text{cm}^2$ for seed pulse durations of 13 fs (a), (b) and 80 fs (c), (d). (a) The Poynting projection of the seed at its maximum amplification ($x = 1000\ k_0^{-1}$). (b) The maximum seed intensity (blue) as a function of its position in the trapezoidal plasma profile (red). Note that the pump enters always from the left ($x = 0\ k_0^{-1}$) and the seed from the right ($x = 5000\ k_0^{-1}$). (c) The Poynting projection of the seed at the beginning, in the middle and at the end of the plasma amplifier. (d) The maximum seed intensity (blue) as a function of its position in the ramp profile (red). In this case the amplification process takes place almost exclusively over a $670\ \mu\text{m}$ downward density ramp from $0.07\ n_c$ to zero, improving stability and efficiency with respect to the configuration presented in (a), (b).

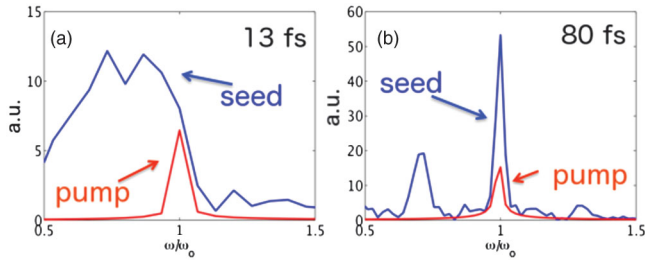


FIG. 3 (color). Spectra of the amplified seed pulses in vacuum for the 13 fs (a) and 80 fs (b) case. The pump pulse spectrum (red) is given for reference.

short pulse it can not be excluded that contributions from QBRA (quasitransient backward Raman amplification [9]) regime are present. Note that the frequency spread of the amplified 13 fs pulse can not be explained by the natural width of the pulse which is of the order $\sim 0.22\omega_0$. This is in contrast to the 80 fs pulse. The spectrum, Fig. 3(b), shows a peak at ω_0 (resolution does not allow us to distinguish between the downshifted peak and the main pump frequency as the difference is of the order of $10^{-3}\omega_0$) as was also found in previous simulations [6]. The underlying mechanism is sc-SBS for the whole amplification process. The peak located at $\sim 0.7\omega_0$ represents a thermal SRS contribution, independent of the presence of the seed. A complementary analysis of the Fourier spectra of the ion and electron densities [21] confirms this scenario. Optimization is possible by tuning the profile of the plasma amplifier. The strategy here is to operate in a regime where SBS is favored while SRS is strongly damped. Since the SRS instability is in general favoured by homogeneous and dense plasmas, this points to the use of ramped density profiles for the amplifier. It has been recently shown that they can be easily generated from gas jets [23]. Ramped plasma profiles have already been used in the context of SRS amplification [8,19,24]. For SRS the gradient scale length is very long: a few 10% density variation over $\sim 500 \mu\text{m}$. It is intended to compensate the chirp present in pump and/or seed in order to uphold the resonance condition. In our case the density varies several 100% over a comparable distance, thus rendering the excitation of thermal SRS by the pump unfavorable.

The use of such profiles was tested successfully in the simulations by comparing three types of profiles: plateau, single ramp [as in Fig. 2(d)], and plateau with ramps at the edges [as in Fig. 2(b)]. The comparison reveals that for the ramp profile [Figs. 2(c) and 2(d)] the SBS energy transfer efficiency is improved, increasing from the original 31% to 53% ($\sim 53 \text{ mJ}$). The seed pulse compression is not affected by switching from the trapezoidal profile to the ramp profile, nor is the final intensity. The energy transfer increase is attributed to two effects. On the one side a reduction of thermal SRS scattering is observed. On the other side the coupling pump seed is improved as the original present modulation (onset of filamentation) of

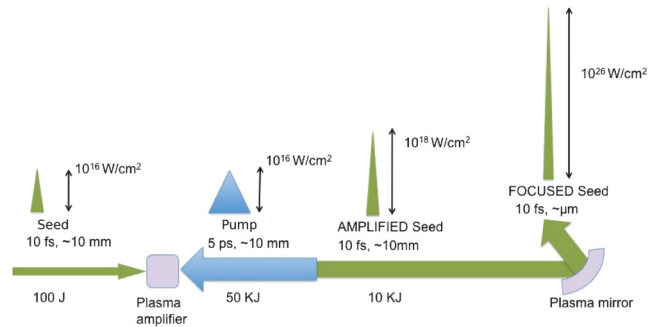


FIG. 4 (color). Diagram showing the combination of compression, amplification and focusing techniques for a high-energy scenario.

the pump has disappeared. It also shows that it is important to have the pump and seed pulses meet at the high-density edge of the ramp with the seed going down the ramp, so that the coupling coefficient is strongest at the beginning of the amplification. Doubling the transverse size of pump and seed in this ramp configuration allows correspondingly more energy to be transferred, $\sim 100 \text{ mJ}$, without affecting the final intensity.

All these optimization strategies can be envisioned to be exploited using present-day facilities as, e.g., the one at LULI where beam lines of short-pulse (30 fs) lasers of low energy are being developed to be available together with longer ones ($> 400 \text{ fs}$) of high energy (20 J) [25]. This would allow testing the schemes explored numerically in the present study, and achieve plasma amplification of such short pulses to the few Joules level, i.e., at a level equivalent to what commercially available lasers [26] can achieve. Beyond such initial step, the interest of the plasma technique is that it offers the prospect of pushing the technique to extreme levels. Using again available facilities, one can indeed already envision the generation of exawatt laser pulses by producing seed pulses with energies around several tens of kJ. For this, as filamentation of neither pump nor seed pulse intervenes, the diameter of the interacting pulses can be increased. As illustrated in Fig. 4, such a high-energy scenario would be as follows. The pump pulse is CPA created with duration 5 ps, energy $\sim 50 \text{ kJ}$ (based on the L-FEX technology [27]), and transverse size of $\sim 10 \text{ mm}$, so that its intensity is $\sim 10^{16} \text{ W/cm}^2$. The seed pulse has a 10 fs duration and an intensity of around 10^{16} W/cm^2 (corresponding to an energy of 100 J, e.g., produced by Apollon-type lasers [28]). Over a plasma length of 2 mm, taking into account a modest extraction efficiency of 20%, a seed of similar duration and intensity of the order 10^{18} W/cm^2 , with an energy of 10 kJ can be produced. The energy that has to be used to ionize and heat to a few hundred eV the $0.05 n_c$ plasma amplifier (of volume $\sim 100 \text{ mm}^3$) is less than 1 kJ. Upon focusing such an exawatt light pulse with a plasma mirror [29] the intensity would increase by a factor 10^8 , i.e., to 10^{26} W/cm^2 . This would provide a way to

overcome existing technological limits [3,30,31], opening up the way to investigate new physics issues such as radiation damping, pair creation, weakly coupled dark fields [32] and make possible fundamental tests of the quantum nature of vacuum [33,34].

Usage of the computing center CCRT of the CEA is acknowledged. C.R. acknowledges support from Grant No. ANR-11-IDEX-0004-02 Plas@Par. The authors thank A. Héron for using the EMI2D PIC-code and D. Pesme and T. Tajima for helpful discussions.

-
- [1] G. A. Mourou and T. Tajima, *Science* **331**, 41 (2011).
- [2] P. B. Corkum and F. Krausz, *Nat. Phys.* **3**, 381 (2007).
- [3] D. Strickland and G. A. Mourou, *Opt. Commun.* **56**, 219 (1985).
- [4] I. N. Ross, in *Strong Field Laser Physics*, edited by T. Brabee (Springer, New York, 2008).
- [5] B. C. Stuart, M. D. Feit, A. M. Rubenchik, B. W. Shore, and M. D. Perry, *Phys. Rev. Lett.* **74**, 2248 (1995).
- [6] A. A. Andreev, C. Riconda, V. T. Tikhonchuk, and S. Weber, *Phys. Plasmas* **13**, 053110 (2006).
- [7] V. M. Malkin, G. Shvets, and N. J. Fisch, *Phys. Rev. Lett.* **82**, 4448 (1999).
- [8] V. M. Malkin, G. Shvets, and N. J. Fisch, *Phys. Rev. Lett.* **84**, 1208 (2000).
- [9] V. M. Malkin and N. J. Fisch, *Phys. Rev. E* **80**, 046409 (2009).
- [10] B. Ersfeld and D. Jaroszynski, *Phys. Rev. Lett.* **95**, 165002 (2005).
- [11] J. Ren, W. Cheng, S. Li, and S. Suckewer, *Nat. Phys.* **3**, 732 (2007).
- [12] R. M. G. M. Trines, F. Fiúza, R. Bingham, R. A. Fonseca, L. O. Silva, R. A. Cairns, and P. A. Norreys, *Phys. Rev. Lett.* **107**, 105002 (2011).
- [13] R. M. G. M. Trines, F. Fiúza, R. Bingham, R. A. Fonseca, L. O. Silva, R. A. Cairns, and P. A. Norreys, *Nat. Phys.* **7**, 87 (2011).
- [14] L. Lancia *et al.*, *Phys. Rev. Lett.* **104**, 025001 (2010).
- [15] International Zetawatt Exawatt Science Technology, <http://www.izest.polytechnique.edu>.
- [16] G. A. Mourou, N. J. Fisch, V. M. Malkin, Z. Toroker, E. A. Khazanov, A. M. Sergeev, T. Tajima, and B. Le Garrec, *Opt. Commun.* **285**, 720 (2012).
- [17] C. E. Max, J. Arons, and A. B. Langdon, *Phys. Rev. Lett.* **33**, 209 (1974).
- [18] D. W. Forslund, J. M. Kindel, and E. L. Lindman, *Phys. Fluids* **18**, 1002 (1975).
- [19] N. A. Yampolsky, N. J. Fisch, V. M. Malkin, E. J. Valeo, R. Lindberg, J. Wurtele, J. Ren, S. Li, A. Morozov, and S. Suckewer, *Phys. Plasmas* **15**, 113104 (2008); N. A. Yampolsky and N. J. Fisch, *Phys. Plasmas* **18**, 056711 (2011).
- [20] C. K. Birdsall and A. B. Langdon, *Plasma Physics via Computer Simulation* (Adam Hilger, Bristol, England, 1991).
- [21] C. Riconda *et al.* (to be published).
- [22] G. Lehmann, F. Schluck, and K. H. Spatschek, *Phys. Plasmas* **19**, 093120 (2012).
- [23] K. Schmid, A. Buck, C. M. S. Sears, J. M. Mikhailova, R. Tautz, D. Herrmann, M. Geissler, F. Krausz, and L. Veisz, *Phys. Rev. ST Accel. Beams* **13**, 091301 (2010).
- [24] Z. Toroker, V. M. Malkin, A. A. Balakin, G. M. Fraiman, and N. J. Fisch, *Phys. Plasmas* **19**, 083110 (2012).
- [25] J. P. Zou, C. L. Blanc, P. Audebert, S. Janicot, A. M. Sautivet, L. Martin, C. Sauteret, J. L. Paillard, S. Jacquemot, and F. Amiranoff, *J. Phys. Conf. Ser.* **112**, 032021 (2008).
- [26] <http://www.amplitude-technologies.com>.
- [27] J. Kawanaka *et al.*, *J. Phys. Conf. Ser.* **112**, 032006 (2008).
- [28] G. Chériaux *et al.*, *AIP Conf. Proc.* **1462**, 78 (2012).
- [29] M. Nakatsutsumi, A. Kon, S. Buffechoux, P. Audebert, J. Fuchs, and R. Kodama, *Opt. Lett.* **35**, 2314 (2010).
- [30] A. Dubietis, G. Jonušauskas, and A. Piskarskas, *Opt. Commun.* **88**, 437 (1992).
- [31] G. A. Mourou, C. P. J. Barry, and M. D. Perry, *Phys. Today* **51**, No. 1, 22 (1998).
- [32] K. Homma, *Prog. Theor. Exp. Phys.* (2012) 04D004.
- [33] G. A. Mourou, T. Tajima, and S. V. Bulanov, *Rev. Mod. Phys.* **78**, 309 (2006).
- [34] Y. I. Salamin, S. X. Hu, K. Z. Hatsagortsyan, and C. H. Keitel, *Phys. Rep.* **427**, 41 (2006).